arXiv:1402.6832v1 [cond-mat.quant-gas] 27 Feb 2014

Gapless topological Fulde-Ferrell superfluidity in spin-orbit coupled Fermi gases

Ye Cao[1,2], Shu-Hao Zou[3], Xia-Ji Liu[1], Su Yi[3], Gui-Lu Long[2,4,5], and Hui Hu[1*]
[1] *Centre for Quantum and Optical Science, Swinburne University of Technology, Melbourne 3122, Australia*
[2] *State Key Laboratory of Low-dimensional Quantum Physics and Department of Physics, Tsinghua University, Beijing 100084, P. R. China*
[3] *State Key Laboratory of Theoretical Physics, Institute of Theoretical Physics, Chinese Academy of Sciences, Beijing 100190, P. R. China*
[4] *Collaborative Innovation Center of Quantum Matter, Beijing 100084, P. R. China and*
[5] *Tsinghua National Laboratory for Information Science and Technology, Beijing 100084, P. R. China*
(Dated: February 28, 2014)

Topological superfluids usually refer to a superfluid state which is gapped in the bulk but metallic at the boundary. Here we report that a gapless, topologically non-trivial superfluid with inhomogeneous Fulde-Ferrell pairing order parameter can emerge in a two-dimensional spin-orbit coupled Fermi gas, in the presence of both in-plane and out-of-plane Zeeman fields. The Fulde-Ferrell pairing - induced by the spin-orbit coupling and in-plane Zeeman field - is responsible for this gapless feature. The existence of such an exotic superfluid is not restricted to the pure Rashba or Dresselhaus spin-orbit coupling. However, its phase space becomes extremely narrow when the spin-orbit coupling is tuned towards having an equal weight in Rashba and Dresselhaus components.

PACS numbers: 05.30.Fk, 03.75.Hh, 03.75.Ss, 67.85.-d

Over the past few years, exotic pairing mechanism has gained widespread concern, making it spring up in a wide range of areas from astrophysics, solid-state physics to ultracold atomic physics, to name a few [1–5]. The spatially modulated Fulde-Ferrell-Larkin-Ovchinnikov (FFLO) state plays a key role in this mechanism [6, 7] and could emerge in spin-imbalanced systems, in which the Bardeen-Cooper-Schrieffer (BCS) state may become unstable against the pairing with finite center-of-mass momentum. Taking the advantage of high controllability [8, 9], ultracold atomic Fermi gases are ideal table-top systems for pursuing the FFLO state [10–12]. Indeed, strong evidence for FFLO superfluidity has been seen in a Fermi cloud of ^{6}Li atoms confined in one dimensional harmonic traps [4, 13, 14]. Most recently, motived by the realization of synthetic spin-orbit coupling (SOC) in cold atoms [15–17], FF superfluidity is also argued to be observable in spin-orbit coupled atomic Fermi gases [18–20]. It is induced by the combined effect of SOC and in-plane Zeeman field, which leads to the deformation of the Fermi surfaces [21–23].

Topological insulators and superconductors have been another hot research area in recent years [24, 25]. These materials are gapped in the bulk but metallic at the boundary, supporting the prerequisites of some crucial physical realities, for example, the non-Abelian anyons used to form quantum gates in fault-tolerant quantum computation [26]. It is now widely believed that topological superconductors (or superfluids) could acquire zero-energy edge states known as Majorana fermions - non-Abelian particles that are their own antiparticles - which are still mysterious and not observed distinctly in recent experiments [27–29]. First proposed to be realizable in chiral p-wave superconductors, Majorana fermions could also exist in s-wave superconductors with SOC [30–33].

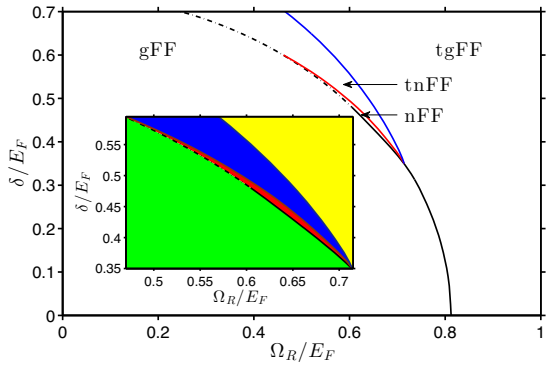

FIG. 1: (Color online) Zero temperature phase diagram of a Rashba spin-orbit coupled 2D Fermi gas at $E_b = 0.5E_F$ and $\lambda = E_F/k_F$. With increasing the out-of-plane Zeeman field Ω_R at a given in-plane field δ, the Fermi superfluid may evolve from a gapped FF (gFF, green) to a nodal FF (nFF, red), then a gapless topological FF (tnFF, blue), and finally to a gapped topological FF (tgFF, yellow). The inset shows an enlarged view near $\Omega_R \simeq 0.6E_F$ and $\delta \simeq 0.5E_F$. The dot-dashed and solid lines correspond to the first- and second-order phase transition boundaries, respectively.

In the context of ultracold atomic Fermi gases, there are already some theoretical works detailing the emergence and stability of topological superfluids in the presence of an out-of-plane Zeeman field [34–36]. Interestingly, topological order is compatible with inhomogeneous FF superfluidity [37–40]. In the case of a two-dimensional (2D) atomic Fermi gas with Rashba SOC and both in-plane and out-of-plane Zeeman fields, a gapped topological FF superfluid has been predicted very recently [39, 40].

In this work, we report the emergence of *gapless* topological FF superfluid in the same 2D setting, as indicated by the "tnFF" phase in Fig. 1, which intervenes between

the topologically trivial (gFF or nFF) and the gapped topologically non-trivial FF states (tgFF), and occupies a sizable parameter space. Furthermore, its existence is not restricted to the pure Rashba or Dresselhaus SOC. Any type of SOC with an unequal weight in the Rashba and Dresselhaus components can support such an exotic gapless topological FF superfluid (see Fig. 5). These findings are remarkable, as commonly topological superfluids are believed to have an energy gap in the bulk [24, 25]. Here our goal is to understand why the gapless energy structure appears and coexists with the topological order, over a broad range of parameters. Understanding this may shed lights on designing new gapless topological materials in solid-state systems.

We emphasize that the emergence of a gapped topological FF superfluid [39, 40], on the contrary, is straightforward to understand. As discussed in the previous work [20, 22], the finite momentum pairing in spin-orbit coupled Fermi gases is induced by an in-plane Zeeman field. A gapped FF superfluid is a continuous evolution of its counterpart without the in-plane field and both two superfluids have similar dispersion relation [38]. The latter can undergo the topological phase transition when an out-of-plane Zeeman field is applied above a threshold [30–33]. In contrast, the gapless topological FF superfluid that we focus on has no such a simple correspondence and we must take into account its non-trivial gapless dispersion relation.

We start by considering the model Hamiltonian of a 2D spin-orbit coupled two-component Fermi gas with the SOC $\lambda_x\hat{k}_x\sigma_x+\lambda_y\hat{k}_y\sigma_y$, the in-plane ($\delta$) and out-of-plane ($\Omega_R$) Zeeman fields, $\mathcal{H}=\int d\mathbf{r}[\mathcal{H}_0+\mathcal{H}_{int}]$, where $\mathcal{H}_0$ is the single-particle Hamiltonian,

$$\mathcal{H}_0=\left[\psi_\uparrow^\dagger(\mathbf{r}),\psi_\downarrow^\dagger(\mathbf{r})\right]\left[\begin{array}{cc}\xi_{\mathbf{k}+} & \Lambda_{\mathbf{k}+}^\dagger\\ \Lambda_{\mathbf{k}+} & \xi_{\mathbf{k}-}\end{array}\right]\left[\begin{array}{c}\psi_\uparrow(\mathbf{r})\\ \psi_\downarrow(\mathbf{r})\end{array}\right], \quad (1)$$

and $\mathcal{H}_{int}=U_0\psi_\uparrow^\dagger(\mathbf{r})\psi_\downarrow^\dagger(\mathbf{r})\psi_\downarrow(\mathbf{r})\psi_\uparrow(\mathbf{r})$ is the interaction Hamiltonian with a pairwise contact interaction of strength U_0. Here we have used the notations, $\xi_{\mathbf{k}\pm}\equiv\hat{\xi}_{\mathbf{k}}\pm\Omega_R\equiv-\hbar^2\nabla^2/(2m)-\mu\pm\Omega_R$ with the atomic mass m and chemical potential μ, and $\Lambda_{\mathbf{k}\pm}\equiv\lambda_x\hat{k}_x+i\lambda_y\hat{k}_y\pm\delta$, where $\hat{k}_x=-i\hbar\partial_x$ and $\hat{k}_y=-i\hbar\partial_y$ are momentum operators. $\psi_\sigma^\dagger(\mathbf{r})$ ($\psi_\sigma(\mathbf{r})$) is the field operator for creating (annihilating) an atom with pseudo-spin state $\sigma\in(\uparrow,\downarrow)$ at $\mathbf{r}$. We have explicitly adopted a general form of SOC including both Rashba (i.e., $\lambda_x=\lambda_y$) and Dresselhaus ($\lambda_x=-\lambda_y$) SOCs. In the recent experiments [16, 17], only the SOC with equally weighted Rashba and Dresselhaus components has been realized, by using two counter-propagating Raman laser beams. The in-plane (δ) and out-of-plane (Ω_R) Zeeman fields can be created depending on the detailed experimental realization of synthetic SOC. In current experiments [16, 17], they correspond to the two-photon detuning and Rabi frequency of the laser beams, respectively. In the interaction Hamiltonian, the bare interaction strength U_0 is to be regularized as $U_0^{-1}=-\mathcal{S}^{-1}\sum_{\mathbf{k}}1/(E_b+\hbar^2\mathbf{k}^2/m)$, where $\mathcal{S}$ is the area of the system and E_b is the two-particle binding energy that physically characterizes the interaction strength.

In the presence of an in-plane Zeeman term $\delta\sigma_x$ in the Hamiltonian, it is known that a finite momentum pairing will arise along the x-direction [20]. Focusing on a FF-like order parameter $\Delta(\mathbf{r})=-U_0\langle\psi_\downarrow(\mathbf{r})\psi_\uparrow(\mathbf{r})\rangle=\Delta e^{iqx}$ at the mean-field level, the interaction Hamiltonian can be approximated by $\mathcal{H}_{int}\simeq-[\Delta(\mathbf{r})\psi_\uparrow^\dagger(\mathbf{r})\psi_\downarrow^\dagger(\mathbf{r})+\text{H.c.}]-|\Delta(\mathbf{r})|^2/U_0$. By introducing the Nambu spinor $\Phi(\mathbf{r})\equiv[\psi_\uparrow,\psi_\downarrow,\psi_\uparrow^\dagger,\psi_\downarrow^\dagger]^T$, the total Hamiltonian can be rewritten in a compact form, $\mathcal{H}=(1/2)\int d\mathbf{r}\Phi^\dagger(\mathbf{r})\mathcal{H}_{BdG}\Phi(\mathbf{r})-\mathcal{S}\Delta^2/U_0+\sum_{\mathbf{k}}\hat{\xi}_{\mathbf{k}}$, where $\mathcal{H}_{BdG}$ is given by,

$$\mathcal{H}_{BdG}\equiv\left[\begin{array}{cccc}\xi_{\mathbf{k}+} & \Lambda_{\mathbf{k}+}^\dagger & 0 & -\Delta(\mathbf{r})\\ \Lambda_{\mathbf{k}+} & \xi_{\mathbf{k}-} & \Delta(\mathbf{r}) & 0\\ 0 & \Delta^*(\mathbf{r}) & -\xi_{\mathbf{k}+} & \Lambda_{\mathbf{k}-}\\ -\Delta^*(\mathbf{r}) & 0 & \Lambda_{\mathbf{k}-}^\dagger & -\xi_{\mathbf{k}-}\end{array}\right]. \quad (2)$$

It is straightforward to diagonalize the above Bogoliubov Hamiltonian $\mathcal{H}_{BdG}\Phi_{\mathbf{k}\eta}^\nu(\mathbf{r})=E_{\mathbf{k}\eta}^\nu\Phi_{\mathbf{k}\eta}^\nu(\mathbf{r})$ with quasiparticle energy $E_{\mathbf{k}\eta}^\nu$ and quasiparticle wave-function $\Phi_{\mathbf{k}\eta}^\nu(\mathbf{r})=1/\sqrt{\mathcal{S}}e^{i\mathbf{k}\cdot\mathbf{r}}[u_{\eta\uparrow}^\nu e^{+iqx/2},u_{\eta\downarrow}^\nu e^{+iqx/2},v_{\eta\uparrow}^\nu e^{-iqx/2},v_{\eta\downarrow}^\nu e^{-iqx/2}]^T$, where $\nu\in(+,-)$ represents the particle ($+$) or hole ($-$) branch, and $\eta\in$(1,2) denotes the upper (1) or lower (2) helicity branch [41]. The mean-field thermodynamic potential Ω at the temperature T is then given by,

$$\Omega=\frac{1}{2}\sum_{\mathbf{k}}\left(\xi_{\mathbf{k}+\mathbf{q}/2}+\xi_{\mathbf{k}-\mathbf{q}/2}\right)-\frac{1}{2}\sum_{\mathbf{k}\eta}|E_{\mathbf{k}\eta}^{\nu=+}|$$
$$-k_BT\sum_{\mathbf{k}\eta}\ln\left(1+e^{-|E_{\mathbf{k}\eta}^{\nu=+}|/k_BT}\right)-\mathcal{S}\frac{\Delta^2}{U_0}, \quad (3)$$

where $\xi_{\mathbf{k}\pm\mathbf{q}/2}=\hbar^2(\mathbf{k}\pm\mathbf{q}/2)^2/(2m)-\mu$. Taking the advantage of inherent particle-hole symmetry in the Nambu spinor representation [20], only the eigenvalues in the particle branch ($\nu=+$) is necessary in the calculation of the thermodynamic potential. For a given set of parameters (i.e., the temperature T, binding energy E_b etc.), different mean-field phases can be determined using the self-consistent stationary conditions: $\partial\Omega/\partial\Delta=0$, $\partial\Omega/\partial q=0$, as well as the conservation of total atom number, $N=-\partial\Omega/\partial\mu$. At a given temperature, the ground state has the lowest free energy $F=\Omega+\mu N$. Hereafter we set the Fermi wavevector $k_F=\sqrt{4\pi N/\mathcal{S}}$ and Fermi energy $E_F=\hbar^2k_F^2/(2m)$ as the units for wavevector and energy, respectively. In all self-consistent calculations, the interaction parameter is given by $E_b=0.5E_F$ and the SOC strength is determined by $\lambda=\sqrt{\lambda_x^2+\lambda_y^2}=E_F/k_F$. For simplicity, we only report the results at zero temperature.

Fig. 1 presents the typical phase diagram for a Rashba spin-orbit coupled 2D Fermi gas on the $\Omega_R-\delta$ plane. The

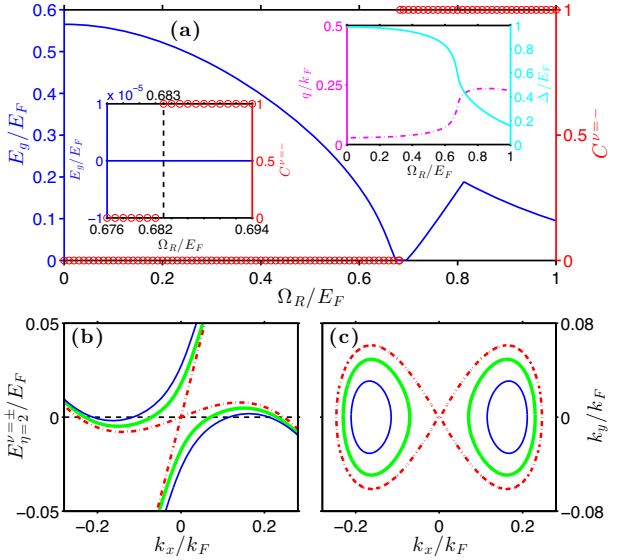

FIG. 2: (Color online) (a) Evolution of the minimum excitation gap E_g and of the Chern number with increasing Ω_R at a fixed $\delta = 0.4E_F$. The left inset is an enlarged view in the gapless region. The right inset shows the evolution of the FF pairing momentum q and pairing gap Δ. (b) Dispersion relation of the lower helicity branch $E^{\nu}_{\eta=2}(k_x, k_y = 0)$ across the topological transition at $\Omega_R/E_F = 0.678$ (green thick line), 0.683 (red dot-dashed line) and 0.693 (blue thin line). (c) The corresponding contours of zero-energy energy spectrum (nodal points) on the k_x-k_y plane.

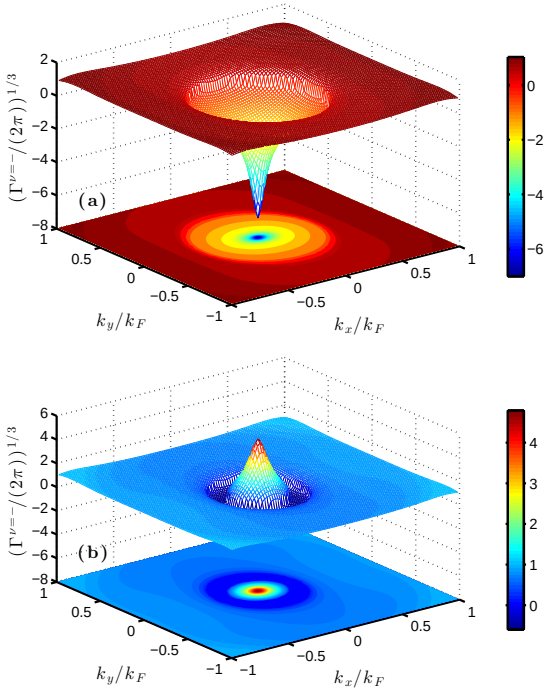

FIG. 3: (Color online) Contour plots of the Berry curvature $\Gamma^{\nu=-} \equiv \gamma_1^{\nu=-} + \gamma_2^{\nu=-}$ before (a, $\Omega_R = 0.678E_F$) and after (b, $\Omega_R = 0.693E_F$) the topological phase transition at an in-plane field $\delta = 0.4E_F$. For better illustration, we show $(\Gamma^{\nu})^{1/3}$ instead of Γ^{ν}.

case of zero in-plane Zeeman field ($\delta = 0$) has been well explored in the literature [30–33]. A topological phase transition is driven by the out-of-plane Zeeman field Ω_R. The increase of Ω_R will not only change the topology of the dispersion relation of two helicity branches via breaking time-reversal symmetry and opening a spin-orbit gap, but it also induce an effective p-wave fermionic pairing in the lower helicity branch [30]. As a result, a gapped topological superfluid emerges continuously above the threshold $\Omega_{R,c} = \sqrt{\mu^2 + \Delta^2}$. Associated with this topological phase transition, the energy gap of the system will first close exactly at $\Omega_{R,c}$ and then immediately re-open. The presence of a nonzero but small in-plane field will not change this picture, but the in-plane field facilitates the finite-momentum FF pairing due to the Fermi surface deformation in the lower helicity branch [20]. Consequently, a gapped topological FF superfluid appears, as discussed in the previous work [39, 40].

It is appealing to perceive, however, that a *gapless* topological FF superfluid can also emerge at the sufficiently large in-plane Zeeman field $\delta \gtrsim 0.35E_F$. In this case, with increasing Ω_R the Fermi gas is first driven into a gapless state before finally turns into a gapped topological superfluid, as can be clearly seen in Fig. 2(a), where we plot the evolution of the minimum excitation gap. In the gapless state, the energy of the lower helicity particle branch ($E^{\nu=+}_{\eta=2}$) becomes less than zero in a small area slightly away from the origin $\mathbf{k} = 0$, as shown in Fig. 2(b). The nodal points with $E^{\nu}_{\eta=2}(k_x, k_y) = 0$ form two disjoint loops in the momentum space, see for example Fig. 2(c), except at a critical value Ω_R, where the two loops connect at $\mathbf{k} = 0$. At this value, the topology of the Fermi surface changes, implying the emergence of a gapless topological FF superfluid.

To better characterize the topological phase transition in the gapless state, we calculate the Chern number

$$C^{\nu=-} = \frac{1}{2\pi} \int d^2\mathbf{k} \sum_{\eta=1,2} \gamma_\eta^{\nu=-} \tag{4}$$

associated with the hole branches ($\nu = -$), where $\gamma_\eta^{\nu} = i(\langle \partial_{k_x} \Phi_\eta^{\nu} | \partial_{k_y} \Phi_\eta^{\nu} \rangle - k_x \leftrightarrow k_y)$ is the Berry curvature of the (ν, η) branch [42]. The results are shown in Fig. 2(a) by circles. The topological state is characterized by a nonzero integer Chern number $C^{\nu=-} = 1$. As anticipated, there is a jump in the Chern number, see for example the left inset of Fig. 2(a), occurring precisely at the critical value Ω_R where the topology of the Fermi surface changes. To gain a concrete understanding of this jump, in Fig. 3 we report the Berry curvature $\Gamma^{\nu=-} \equiv \gamma_1^{\nu=-} + \gamma_2^{\nu=-}$ just before and after the topological phase transition. In either case, a sharp peak develops in the k_x-k_y plane around the origin $\mathbf{k} = 0$, pointing downwards or upwards and sitting on a positive background. In the topologically trivial state, when atoms scatter on

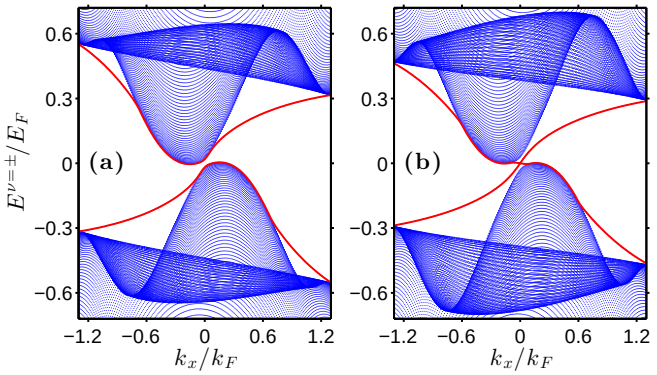

FIG. 4: (Color online) Energy spectrum of a 2D strip formed by imposing open boundary condition (i.e., hard wall confinement) in the y-direction. The edge states due to the confinement are highlighted by the red lines. The parameters are $\delta = 0.4E_F$ and $\Omega_R = 0.678E_F$ (a) or $\Omega_R = 0.693E_F$ (b), the same as in Fig. 3.

the Fermi surface, a Berry phase $\theta = \int d^2\mathbf{k}\Gamma^{\nu=-} \simeq -\pi$ is picked up from the downwards peak but cancels with these accumulated from the background, leading to a vanishing Chern number. In contrast, in the topologically non-trivial state, the two contributions are additive and hence yield a nonzero Chern number $C^{\nu=-} = 1$.

Our gapless topological FF superfluid can support exotic chiral edge modes, like any topological states [24, 25]. To confirm this fundamental feature, in Fig. 4 we report the energy spectrum of a 2D strip with hard-wall confinement in the y-direction. Two sets of chiral edge states appear due to the confinement. In the gapless topological FF state, they come to cross with each other at $k_x = 0$, giving rise to two zero-energy Majorana fermions. We have confirmed numerically that the wavefunctions of the left- and right-moving chiral edge states are indeed well localized at the two boundaries, respectively.

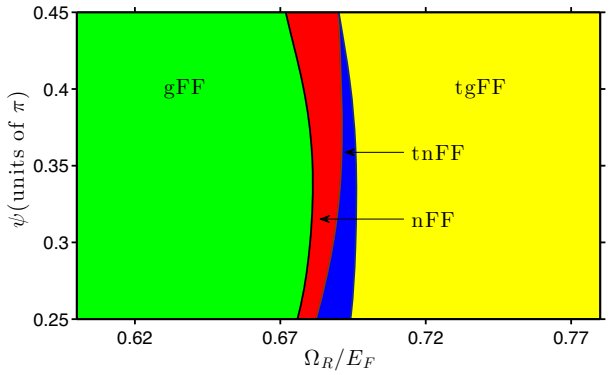

FIG. 5: (Color online) Phase diagram of a 2D Fermi gas with a general SOC on the $\Omega_R - \psi$ plane at $\delta = 0.4E_F$. Here, we define an azimuthal angle $\psi = \arctan(\lambda_y/\lambda_x)$. The parameter space for the gapless topological FF superfluid suppresses away from the Rashba limit (i.e., $\psi = 0.25\pi$).

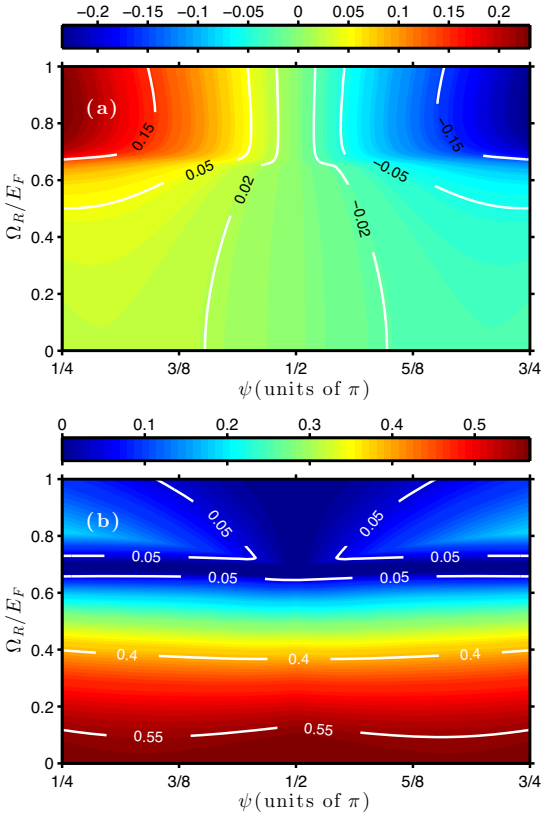

FIG. 6: (Color online) Contour plots of the FF pairing momentum q (a) and of the energy gap E_g (b) on the $\psi - \Omega_R$ plane at $\delta = 0.4E_F$. Note that, when $\psi \to \pi - \psi$, the pairing momentum $q \to -q$ and the energy gap remains unchanged.

We note that in the phase diagram Fig. 1, with increasing the in-plane Zeeman field δ the parameter space of the gapless topological FF superfluid (labelled as "tnFF") would become larger. In addition, different competing gapless solutions may exist. This leads to a first-order phase transition between the gapped and gapless FF superfluids, as indicated by the dot-dashed line in Fig. 1.

We now turn to consider a general SOC characterized by $\lambda_x = \lambda\cos\psi$ and $\lambda_y = \lambda\sin\psi$. Fig. 5 presents the zero-temperature phase diagram when the SOC is tuned away from the Rashba limit ($\lambda_x = \lambda_y$ or $\psi = \pi/4$) and Fig. 6 summarizes the corresponding FF pairing momentum and energy gap. Remarkably, the gapless topological FF superfluid (i.e., blue area) survives over a broad range of the azimuthal angle ψ. This observation is encouraging, as the synthetic SOC - to be experimentally realized in cold-atom laboratories - may not acquire the perfect form of a Rashba SOC. The insensitive dependence of the gapless topological FF superfluid on a particular form of SOC therefore means that this conceptually new topological state of matter is amenable to synthesize with cold atoms. We note that towards an equal weight combination of Rashba and Dresselhaus SOCs ($\psi = \pi/2$), the FF pairing momentum decreases to zero as a result of

$\lambda_x = 0$, as shown in Fig. 6(a). In this limit, all the topological states, gapless or gapped, vanish identically, as one may anticipate.

In summary, we have predicted a gapless topological superfluid with inhomogeneous Fulde-Ferrell pairing in a two-dimensional spin-orbit coupled Fermi gas, which possesses gapless excitations in the bulk as well as non-Abelian Majorana fermions localized at the boundary. It exists over a wide range of parameters and does not require specific form of spin-orbit coupling, and is therefore feasible to observe experimentally in cold-atom laboratories. The gapless excitation in the bulk would lead to richer thermodynamic and dynamic properties of the system. However, as a trade-off our gapless topological Fulde-Ferrell superfluid may not have the same stability as conventional gapped topological superfluid, since the zero-energy Majorana fermions is no longer protected by a nonzero energy gap. In three dimensions, the proposed gapless topological phase may get larger parameter space, as the gapless feature is favored by high dimensionality. We hope our work would shed new insights for the exploration of topological quantum matters, in both cold-atom and solid-state systems.

This research is supported by the ARC Discovery Projects (FT130100815, DP140103231 and DP140100637), NFRP-China (2011CB921502 and 2011CB921602) and NSFC-China (11025421, 11228410, 11175094 and 91221205).

Note added. — In completing this work, we become aware of a related work [43], where the gapless topological Fulde-Ferrell superfluid in three dimensions is discussed.

* Electronic address: hhu@swin.edu.au

[1] R. Casalbuoni and G. Nardulli, Rev. Mod. Phys. **76**, 263 (2004).

[2] S. Uji, T. Terashima, M. Nishimura, Y. Takahide, T. Konoike, K. Enomoto, H. Cui, H. Kobayashi, A. Kobayashi, H. Tanaka, M. Tokumoto, E. S. Choi, T. Tokumoto, D. Graf, and J. S. Brooks, Phys. Rev. Lett. **97**, 157001 (2006).

[3] M. Kenzelmann, Th. Strässle, C. Niedermayer, M. Sigrist, B. Padmanabhan, M. Zolliker, A. D. Bianchi, R. Movshovich, E. D. Bauer, J. L. Sarrao, and J. D. Thompson, Science **321**, 1652 (2008).

[4] Y.-A. Liao, A. S. C. Rittner, T. Paprotta, W. Li, G. B. Partridge, R. G. Hulet, S. K. Baur, and E. J. Mueller, Nature (London) **467**, 567 (2010).

[5] S. Gerber, M. Bartkowiak, J. L. Gavilano, E. Ressouche, N. Egetenmeyer, C. Niedermayer, A. D. Bianchi, R. Movshovich, E. D. Bauer, J. D. Thompson, and M. Kenzelmann, Nature Phys. **10**, 126 (2014).

[6] P. Fulde and R. A. Ferrell, Phys. Rev. **135**, A550 (1964).

[7] A. I. Larkin and Y. N. Ovchinnikov, Zh. Eksp. Teor. Fiz. **47**, 1136 (1994) [Sov. Phys. JETP **20**, 762 (1965)].

[8] M. W. Zwierlein, A. Schirotzek, C. H. Schunck, and W. Ketterle, Science **311**, 492 (2006).

[9] G. B. Partridge, W. Li, R. I. Kamar, Y.-A. Liao, and R. G. Hulet, Science **311**, 503 (2006).

[10] D. E. Sheehy and L. Radzihovsky, Phys. Rev. Lett. **96**, 060401 (2006).

[11] H. Hu and X.-J. Liu, Phys. Rev. A **73**, 051603(R) (2006).

[12] K. B. Gubbels and H. T. C. Stoof, Phys. Rep. **512**, 255 (2013).

[13] G. Orso, Phys. Rev. Lett. **98**, 070402 (2007).

[14] H. Hu, X.-J. Liu, and P. D. Drummond, Phys. Rev. Lett. **98**, 070403 (2007).

[15] Y.-J. Lin, K. Jiménez-García, and I. B. Spielman, Nature (London) **471**, 83 (2011).

[16] P. Wang, Z.-Q. Yu, Z. Fu, J. Miao, L. Huang, S. Chai, H. Zhai, and J. Zhang, Phys. Rev. Lett. **109**, 095301 (2012).

[17] L. W. Cheuk, A. T. Sommer, Z. Hadzibabic, T. Yefsah, W. S. Bakr, and M. W. Zwierlein, Phys. Rev. Lett. **109**, 095302 (2012).

[18] Z. Zheng, M. Gong, X. Zou, C. Zhang, and G.-C. Guo, Phys. Rev. A **87**, 031602(R) (2013).

[19] F. Wu, G.-C. Guo, W. Zhang, and W. Yi, Phys. Rev. Lett. **110**, 110401 (2013).

[20] X.-J. Liu and H Hu, Phys. Rev. A **87**, 051608(R) (2013).

[21] V. Barzykin and L. P. Gor'kov, Phys. Rev. Lett. **89**, 227002 (2002).

[22] L. Dong, L. Jiang, H. Hu, and H. Pu, Phys. Rev. A **87**, 043616 (2013).

[23] V. B. Shenoy, Phys. Rev. A **88**, 033609 (2013).

[24] M. Z. Hasan and C. L. Kane, Rev. Mod. Phys. **82**, 3045 (2010).

[25] X.-L. Qi and S.-C. Zhang, Rev. Mod. Phys. **83**, 1057 (2011).

[26] C. Nayak, S. H. Simon, A. Stern, M. Freedman, and S. Das Sarma, Rev. Mod. Phys. **80**, 1083 (2008).

[27] V. Mourik, K. Zuo, S. M. Frolov, S. R. Plissard, E. P. A. M. Bakkers, and L. P. Kouwenhoven, Science **336**, 1003 (2012).

[28] J. R. Williams, A. J. Bestwick, P. Gallagher, S. S. Hong, Y. Cui, Andrew S. Bleich, J. G. Analytis, I. R. Fisher, and D. Goldhaber-Gordon, Phys. Rev. Lett. **109**, 056803 (2012).

[29] L. P. Rokhinson, X. Liu and J. K. Furdyna, Nature Phys. **8**, 795 (2012).

[30] C. Zhang, S. Tewari, R. M. Lutchyn, and S. Das Sarma, Phys. Rev. Lett. **101**, 160401 (2008).

[31] M. Sato, Y. Takahashi, and S. Fujimoto, Phys. Rev. Lett. **103**, 020401 (2009).

[32] J. D. Sau, R. M. Lutchyn, S. Tewari, and S. Das Sarma, Phys. Rev. Lett. **104**, 040502 (2010).

[33] Y. Oreg, G. Refael, and F. von Oppen, Phys. Rev. Lett. **105**, 177002 (2010).

[34] X.-J. Liu, L. Jiang, H. Pu, and H. Hu, Phys. Rev. A **85**, 021603(R) (2012).

[35] X.-J. Liu and H. Hu, Phys. Rev. A **85**, 033622 (2012).

[36] R. Wei and E. J. Mueller, Phys. Rev. A **86**, 063604 (2012).

[37] C. Chen, Phys. Rev. Lett. **111**, 235302 (2013).

[38] X.-J. Liu and H. Hu, Phys. Rev. A **88**, 023622 (2013).

[39] C. Qu, Z. Zheng, M. Gong, Y. Xu, L. Mao, X. Zou, G. Guo, and C. Zhang, Nat. Comm. **4**, 2710 (2013).

[40] W. Zhang and W. Yi, Nat. Comm. **4**, 2711 (2013).

[41] H. Hu, L. Jiang, X.-J. Liu, and H. Pu, Phys. Rev. Lett. **107**, 195304 (2011).

[42] D. Xiao, M.-C. Chang, and Q. Niu, Rev. Mod. Phys. **82**, 1959 (2010).

[43] Y. Xu, R. Chu, and C. Zhang, arXiv:1310.4100.